Queensland University of Technology
Brisbane Australia

This is the author's version of a work that was submitted/accepted for publication in the following source:

Thurber, A. E., Douglas, G., Sturm, E. C., Zabierowski, S. E., Smit, D. J., Ramakrishnan, S. N., Hacker, Elke, Leonard, J. H, Herlyn, M., & Sturm, R. A. (2011) Inverse expression states of the BRN2 and MITF transcription factors in melanoma spheres and tumour xenografts regulate the NOTCH pathway. *Oncogene*, *30*(27), pp. 3036-3048.

This file was downloaded from: http://eprints.qut.edu.au/47503/

© **Copyright 2011 Macmillan Publishers Limited**

Notice: *Changes introduced as a result of publishing processes such as copy-editing and formatting may not be reflected in this document. For a definitive version of this work, please refer to the published source:*

http://dx.doi.org/10.1038/onc.2011.33

Inverse expression states of the BRN2 and MITF transcription factors in melanoma spheres and tumour xenografts regulate the NOTCH pathway

A.E. Thurber[1], G. Douglas[1], E.C. Sturm[1], S.E. Zabierowski[2], D.J. Smit[1], S.N. Ramakrishnan[1], Elke Hacker[3], J.H. Leonard[3], M. Herlyn[2], R.A. Sturm[1,2,4]

[1]*Institute for Molecular Bioscience, Melanogenix Group, The University of Queensland, Brisbane, Qld 4072, Australia;* [2]*The Wistar Institute, Philadelphia, Pennsylvania 19104,* USA*; and* [3]*Queensland Institute of Medical Research, Brisbane, Qld 4029, Australia.*

Running title: BRN2-MITF regulate NOTCH in melanoma

4 To whom requests for reprints should be addressed, at Institute for Molecular Bioscience, University of Queensland, Brisbane Qld. 4072, Australia. Phone: (61) (7) 3365 1831; Fax: (61) (7) 3365 4388; E-mail: R.Sturm@imb.uq.edu.au

Abstract

The use of adherent monolayer cultures have produced many insights into melanoma cell growth and differentiation, but often novel therapeutics demonstrated to act on these cells are not active in vivo. It is imperative that new methods of growing melanoma cells that reflect growth in vivo are investigated. To this end, a range of human melanoma cell lines passaged as adherent cultures or induced to form melanoma spheres (melanospheres) in stem cell media have been studied to compare cellular characteristics and protein expression. Melanoma spheres and tumours grown from cell lines as mouse xenografts had increased heterogeneity when compared to adherent cells and 3D-spheroids in agar (aggregates). Furthermore, cells within the melanoma spheres and mouse xenografts each displayed a high level of reciprocal BRN2 or MITF expression, which matched more closely the pattern seen in human melanoma tumours *in situ*, rather than the propensity for co-expression of these important melanocytic transcription factors seen in adherent cells and 3D-spheroids. Notably, when the levels of the BRN2 and MITF proteins were each independently repressed using siRNA treatment of adherent melanoma cells, members of the NOTCH pathway responded by decreasing or increasing expression respectively. This links BRN2 as an activator and conversely MITF as a repressor of the NOTCH pathway in melanoma cells. Loss of the BRN2-MITF axis in antisense ablated cell lines decreased melanoma sphere forming capability, cell adhesion during 3D-spheroid formation, and invasion through a collagen matrix. Combined, this evidence suggests that the melanoma sphere culture system induces subpopulations of cells that may more accurately portray the *in vivo* disease, than growth as adherent melanoma cells.

Key words: cell adhesion, invasion, melanoma, metastasis, NOTCH, transcription factor

Introduction

Despite several decades of research on the causes and potential treatments for melanoma, little improvement has been made in the prognosis of this cancer which remains at less than 15% survival after 5 yrs for patients diagnosed with metastatic disease (Miller and Mihm, 2006). One issue slowing progress is the large disparity that often exists between experimental results and clinical outcomes. In order to screen new therapeutic drugs more quickly and cost effectively new culture models representative of the clinical setting are needed. This has lead to a gain in popularity of three-dimensional (3D) culture systems as an alternative to adherent monolayer culture. Fang et. al. 2005 demonstrated that growth of melanoma cell lines in stem cell media to form non-adherent spheres increased their tumorigenic grafting ability, making this an interesting new model to study (Fang *et al.*, 2005). Growth of melanoma spheres was initially developed because it was thought that the stem cell conditions would enrich an otherwise small 'cancer stem cell' population (Schatton *et al.*, 2008). However, recent evidence has dispelled the notion of only a select subpopulation of cancer cells having the ability to form a melanoma tumour (Quintana *et al.*, 2008), making it likely that other unknown factors are responsible for the increased tumorigenesis seen with melanoma sphere formation and growth. As yet, the relationship between the sphere growth characteristics, expression profiles and behaviour in relation to melanoma *in situ* has not been fully investigated.

An important consideration in melanoma treatment is the high degree of heterogeneity found in tumours (Hoek *et al.*, 2008), as clearly illustrated by the inverse expression pattern of two transcription factors, BRN2 and MITF, important in proliferation and metastasis (Carreira *et al.*, 2006; Goodall *et al.*, 2008). These two proteins have been implicated in the regulation of downstream pathways linked to invasive abilities, as has the NOTCH pathway (Pinnix and Herlyn, 2007), but as yet a relationship between these pathways has not been described. In

human melanoma tumour samples BRN2 and MITF mark two distinct subpopulations predicted to have different proliferative and invasive abilities, while in adherent cultures they are seen to be co-expressed. Therefore, the pattern of these two proteins may provide a measure of tumour-like heterogeneity seen using *in vitro* culture systems and have been investigated here using adherent and non-attached melanoma cell growth states.

Results

Media conditions required for melanoma sphere formation

A range of diverse melanoma cell lines including those of known BRAF, NRAS, PTEN gene mutation status (Johansson *et al.*, 2007; Pavey *et al.*, 2004), several with β-catenin mutations, non-pigmented and pigmented strains, four ocular melanomas, and a cell line showing spontaneous sphere growth were available for this study. In all, 31 parental melanoma cell lines (Supplementary Table 1) and several primary melanoblast strains (Cook *et al.*, 2003) were investigated for their ability to form spheres in 3 different types of media using the method first developed by Fang et al. 2005 (Fang *et al.*, 2005). This method utilized stem cell growth conditions with mouse embryo fribroblast (MEF) conditioned media to promote the growth of non-adherent spheres. In addition to standard melanoma (MEL) and stem cell media (hESCM-KSR), we also assayed for sphere growth in stem cell media supplemented with 10% FBS (hESCM-FBS) instead of 20% Knockout Serum Replacement.

Cells were allowed to grow undisturbed in each media for 14 days or until melanoma spheres formed. Melanoblasts were unable to sustain growth in any of these media. Of the melanoma cell lines tested only 16% had the capacity for detached cell growth using MEL media with only a minor increase to 19% seen using hESCM-FBS; however the majority of cell lines, 87% (27 out of 31), were capable of forming non-adherent melanoma spheres when cultured in hESCM-KSR. Morphological differences between cell lines were observed during initial sphere formation. Some lines produced small spheres within the first few days

of culture, while others grew large sheets of cells detaching after 14 days of culture. Two examples showing some of the variation in sphere formation are illustrated using the pigmented A11 (Figure 1A) and the spontaneous sphere forming D10 (Figure 1B) cell lines. Melanoma spheres were harvested and passaged by dissociation into single cell suspensions and replated. After passaging, the melanoma spheres tended to be smaller and to have a more regular globular shape. In agreement with previous data (Fang *et al.*, 2005), some cell lines lost pigmentation during the first few passages in hESCM-KSR media. The A11 cells were initially darkly pigmented when cultured as an adherent monolayer in MEL media and became unpigmented after three serial passages as detached cells in hESCM-KSR media (Figure 1C). Unpigmented sphere cells did not regain pigmentation after culturing as an adherent monolayer for 14 days in MEL media. In contrast this change in pigmentation pattern was not seen in A11 melanoma spheres derived using hESCM-FBS media.

Due to the greater success of sphere formation in hESCM-KSR media, only melanoma spheres generated under these conditions were used for further characterization. To examine changes in protein profiles, we chose to focus our studies on three melanoma cell lines, two BRAF V600E positive cell lines, previously studied extensively in our laboratory, A2058 and MM96L, and one additional pigmented melanoma cell line, A11 expressing a mutant β-catenin protein. All three lines readily formed melanoma spheres.

Regulatory protein changes between adherent and melanoma sphere cultures

Previously, melanoma spheres were shown to establish tumours more readily in a mouse xenograft model than melanoma cells from adherent cultures (Fang *et al.*, 2005). Since we have previously shown that ablation of BRN2 gene expression prevents establishment of melanoma tumour growth in mouse xenografts (Thomson *et al.*, 1995), we were interested to compare BRN2 protein levels in the same cell line under adherent versus melanoma sphere conditions in addition to other transcription factors known to be associated with melanoma

progression. Western blot analysis of total protein extracts prepared from each cells grown adherently or as spheres demonstrated a consistent decrease in the level of BRN2 protein in melanoma spheres generated using all 3 cell lines A2058, A11, and MM96L (Figure 2A). As BRN2 is proposed to repress MITF (Goodall *et al.*, 2008) and induce NOTCH1 (Castro *et al.*, 2006), two potential BRN2 downstream transcription factor targets, we also determined their expression. Both MITF and NOTCH1 protein levels consistently decreased in spheres from all 3 melanoma lines when compared to their adherent counterpart (Figure 2A). There was a similar suppression of the NOTCH ligands DLL1 and JAG2 during melanoma sphere growth.

Assaying of RNA transcript levels in the adherent and melanoma spheres was performed using quantitative RT-PCR as shown by the representative data presented for the MM96L cell line (Figure 2B). This revealed significant reductions in mRNA levels for BRN2, MITF, NOTCH1 and DLL1 in line with the reduction in their protein levels. There was inconsistency between the protein and mRNA responses seen for JAG2, with a decrease in protein but not transcript in MM96L spheres. Notably spheroid growth did not alter the transcript level of the ABCB5 gene, which had previously been described as a cancer initiating cell marker (Schatton *et al.*, 2008).

Given the cell heterogeneity found in melanoma, we were interested to examine the protein expression and localization at a cellular level of several of these proteins using immunofluorescence as well as measuring total protein levels. Cryosections of melanoma spheres were stained and imaged along with matched adherent melanoma cells for comparison. Immunofluoresence microscopy of the three NOTCH pathway proteins seen to be consistently reduced in levels by immunonoblot assay when A2058 cells were grown as melanospheres compared to adherent conditions was undertaken. Adherent cells had strong and homogeneous intracellular cytoplasmic staining patterns for NOTCH1, JAG2 and DLL1

when counterstained with DAPI to highlight the nucleus (Figure 2C). In contrast in the sections prepared from the fixed spheres there was substantially reduced JAG2 signal but no difference in cellular localisation. For NOTCH1 and DLL1 there was diffuse staining in the cytoplasm, with no nuclear staining as seen by the blue colour of the DAPI stain. Areas of stronger and weaker staining intensity were apparent in sections with the cells near the exterior of the sphere tending toward greater expression than those in the middle, but no conclusions could be drawn from the appearance of this distribution, apart from an increased heterogeneity compared to adherent cell growth.

Immunofluorescence microscopy detects reciprocal BRN2 and MITF expression patterns in melanoma spheres and in tumour xenografts

BRN2 and MITF transcription factors have been shown to have different expression patterns in adherent cultures as compared to *in vivo* tumour samples where they have been reported to mark two distinct subpopulations in melanoma biopsies (Carreira *et al.*, 2006; Goodall *et al.*, 2008). For this reason we investigated the expression patterns of these two transcription factors in melanoma spheres. Firstly, examination of adherent cultures of A2058, A11 and MM96L cells costained with anti-BRN2 (red) and anti-MITF antisera (green) by immunofluorescence confirmed that the majority of cells showed a high degree of BRN2-MITF co-expression in the nucleus (colour range yellow to orange, Figure 3) with only a few cells that did not stain with anti-MITF antibody to some degree and no cells lacked BRN2 expression when examined by single channel excitation (data not shown). However, there were a minor number of isolated cells that stained principally with one or the other of these antibodies, appearing predominantly tinged red or green (Figure 3A upper panel). Secondly, costaining of each of these melanoma cell lines when induced to adhere to each other and form a short term 3D spheroid aggregate structure through plating on a non-adherent agar covered tissue culture dish, produced spheres with a predominantly yellow immunofluorescent staining pattern (Figure 3A middle panel). Lastly, in contrast to the

predominant co-expressed staining patterns of BRN2-MITF in the adherent and 3D spheroid aggregate states, melanoma spheres generated from the A2058, A11 and MM96L cell lines all revealed greater levels of heterogeneity and an appearance of reciprocal expression of BRN2 and MITF, with a predominance of cell nuclei being either red or green (Figure 3A lower panel).

To compare the inverse BRN2-MITF immunofluorescent staining pattern obtained using sectioned melanoma spheres with that of melanoma cells grown as tumours in vivo, we sectioned and co-stained melanoma tissue from mouse xenografts (Figure 3B) and human superficial spreading melanoma (Figure 3C). Two metastatic melanoma cell lines WM3734 and WM115 grown either under adherent culture conditions or as melanoma spheres were injected into the dorsal area of immunocompromised mice and allowed to form tumours. The initial culture conditions of either of these cell lines made no difference to the histological appearance seen upon H&E staining of the tumour sections. Moreover, a dichotomous red-green staining pattern of nuclei indicating either BRN2 positive or MITF positive subpopulations of cells was readily apparent in the melanoma tissue derived from both adherent and melanoma sphere derived xenografts. There were surprisingly few cells in these sections giving rise to a yellow costaining signal in nuclei, indicating only a minor component of BRN2-MITF co-expression in the melanoma xenografts, but this did vary slightly between sections being inspected. Of note was the absence of staining within some patches of cells when comparing consecutive sections prepared for H&E or immunofluoresence analysis. This may represent regions of cell necrosis, another subpopulation of BRN2 and MITF negative melanoma cells, or another non-melanoma cell infiltrating or supporting the tumour. Examination of human tumour sections was largely consistent with the predominant red or green nuclei staining pattern of the xenografts, however a slightly increased frequency of yellow nuclei was visible as seen in the highlighted box (Figure 3C).

The major conclusion to be drawn from the immunofluorescent analysis of BRN2-MITF co-stained melanoma tumour sections is that there is a pattern of co-localization of BRN2 and MITF in some areas as well as restricted expression of sub populations as shown by Goodall and colleagues (Goodall *et al.*, 2008).

Repression of BRN2 or MITF shows reciprocal effects on NOTCH pathway members

To determine if direct repression of the BRN2 transcription factor in melanoma cells would influence the mRNA expression of the NOTCH pathway ligand and receptors, the MM96L and A2058 cell lines grown in adherent conditions were treated with non-specific or BRN2 targeted siRNA molecules. Knockdown of the BRN2 protein in melanoma cells using this reagent has previously been demonstrated (Cook *et al.*, 2005), and repression was confirmed by a decrease in total RNA quantitative RT-PCR (Figure 4A and B) and protein (Figure 4C) levels. Notably, assay of the NOTCH1, JAG2 and DLL1 transcripts all showed a significant reduction of expression relative to the non-specific siRNA, concomitant with the knockdown of BRN2 in A2058 cells, and in MM96L cell extracts although the JAG2 transcript level was not altered the protein itself was reduced. In contrast ABCB5 transcript levels were shown to increase upon BRN2 siRNA treatment of both cell lines. For MITF, the transcript level was slightly reduced or unaltered upon BRN2 ablation, while the MITF protein appeared to increase in A2058 cell extracts, a result consistent with that reported previously (Cook and Sturm, 2008; Goodall *et al.*, 2008) as BRN2 is known to act to repress MITF expression. Conducting the reverse experiment with an siRNA to the MITF transcription factor (Newton *et al.*, 2007), confirmed repression of MITF mRNA and demonstrated a significant 2 fold or greater increase of BRN2, NOTCH1, JAG2 transcript levels, with a decrease in ABCB5 as did DLL1 in A2058 cells (Figure 4A and B). The protein levels for BRN2 and NOTCH1 were increased in both cell lines, as was JAG2 in A2058 cell extracts (Figure 4C).

The reciprocal effects of individually repressing these two transcription factors supports the hypothesis (Cook and Sturm, 2008) of opposing regulatory networks operating through these two proteins in melanoma cells both on their own expression (Carreira *et al.*, 2006; Goodall *et al.*, 2008; Thomson *et al.*, 1995), and as demonstrated here on three members of the NOTCH pathway.

Loss of BRN2-MITF expression compromises melanoma sphere formation and growth

To assess the role of the BRN2 and MITF transcription factors in the initial induction and establishment of melanoma sphere growth states, we chose to examine two derived strains molecularly engineered from the melanoma sphere forming MM96L parental cell line. We have previously described the MM96Lc8 and MM96Lc10 clonal derived lines that were established by permanent transfection and selection for expression of a BRN2 antisense RNA construct (Thomson *et al.*, 1995). Both of these cell lines were subsequently shown to consist of two subpopulations that differed morphologically in being dendritic (D) or low contrast (LC) under bright field microscopy, and which retained (D) or ablated (LC) the expression of the BRN2 and MITF proteins, as well as differentially expressing several pigmentation-associated antigens (Cook *et al.*, 2006). These clonal sub-variants MM96Lc8LC and MM96Lc10LC were used to assay the effect on melanoma sphere formation of the loss of the BRN2-MITF axis when compared with the MM96L parental and MM96Lc8D and MM96Lc10D cell lines (Figure 5A). There was little difference between the parental and dendritic cell lines in the number, efficiency, appearance and propagation of the spheres generated when switched to hESCM-KSR media. In disparity both of the low contrast cell lines generated melanoma spheres poorly, with MM96Lc8LC only able to generate small spheres, at an extremely low rate and over much longer time frames (several weeks). The number of spheres forming 11 to 31 days post induction were quantitated by aspiration from the dish and the counts are presented in Figure 5A, where it is clear that MM96Lc10LC was also compromised in its melanoma sphere forming ability.

Each of these cell lines were tested in a 3D spheroid aggregate model where it was clear that the low contrast lines were also unable to adhere to each other and form a compact structure (Figure 5B). Low contrast cells also had a reduced ability to produce outgrowths (invade) through a collagen matrix when propagated as melanoma spheres in comparison to the parental MM96L cell line with MM96Lc8LC showing no outgrowths (Figure 5C). Furthermore, testing of the protein expression profile of these cell lines grown in the adherent or melanoma sphere state revealed contrasting results (Figure 5D). The loss of BRN2-MITF proteins was apparent in extracts prepared from the MM96Lc8LC and MM96Lc10LC cells as either adherent (lanes 5, 9) or as melanoma spheres (lanes 6, 10), as was the loss of the pigmentation markers TYRP1 and DCT. The NOTCH pathway was again disturbed with the BRN2 ablated cells, containing higher levels of NOTCH1 which was not down regulated in the MM96Lc10LC melanoma spheres.

Discussion

The increased ability of a range of melanoma cell lines to form spheres in hESCM-KSR as compared to hESCM-FBS medium indicates that bovine serum may contain inhibitory factors preventing the cells from reacting to stem cell like conditions that may be enhanced during metastatic transformation (Mani *et al.*, 2008). FBS is known to contain growth factors promoting cell attachment as well as differentiation both of which may counteract sphere formation. Another recent study has described the melanoma sphere forming ability of a single melanoma cell line WM-266-4, in which there was reported to be a small endogenous floating population of cells able to assume this state upon serum depletion and growth in neural stem cell-enriched media (Na *et al.*, 2009a). We have also tested this same cell line and found it to form spheres in both types of media using our conditions (Supplementary Table 1). Notably, sphere formation of the WM-266-4 cell line could be promoted by treatment with a specific developmentally staged embryo extract from Zebrafish, possibly through TGF-β like signalling molecules (Na *et al.*, 2009b). Thus,

melanoma sphere formation is directly influenced by the microenvironment the cells are subjected to, with embryonic conditions stimulating the adoption of this state of growth and plasticity (Fang *et al.*, 2005). Switching from epithelial to mesenchymal cell states (EMT) is a major determinant of melanoma metastasis which results in altered cell adhesive, invasive and migratory properties (Alonso *et al.*, 2007; Smit *et al.*, 2007). This is possibly linked to the changes in regulatory proteins accompanying the switch between melanoma cells grown in an adhesive or melanoma sphere states.

A general characteristic of growth as melanoma spheres compared to their adherent growth pattern was the reduction in the levels of the transcription factors assayed including BRN2, MITF, NOTCH1 and the JAG2 and DLL1 ligands. The NOTCH pathway participates in a variety of cellular processes including cell fate specification, proliferation, adhesion, migration and EMT, and more recently has been implicated in conferring a transformed phenotype when expressed in normal human melanocytes (Pinnix *et al.*, 2009) and progression of melanoma to metastasis (Pinnix and Herlyn, 2007). A link between the BRN2-MITF controlled gene network and regulation of the NOTCH pathway as seen with the reciprocal expression level changes upon repression of each molecule (Figure 4) has not previously been reported, but may have been anticipated. BRN2 has been reported to interact with the proneural basic-helix-loop helix transcription factor Mash1 (Castro *et al.*, 2006). This synergistic transcriptional activation occurs via an evolutionarily conserved octamer-E-box motif (termed the Mash1/Brn motif) first identified within the mouse Mash1-specific enhancer of the Delta1 gene, which codes for one of several ligands for the Notch receptor. Using a bioinformatics approach, the co-ordinate Mash1 / Brn motif could be identified in the promoters of 21 other genes, and which also included several other members of the Notch signalling pathway (Castro *et al.*, 2006). Thus BRN2 has been shown to interact with these elements and the presence of the E-Box that is a core element for the MITF target binding site means there are potentially two levels of interaction that may

regulate the NOTCH pathway in melanocytic cells. The first is some direct BRN2-MITF joint interaction on the regulatory region of these genes to result in reciprocal expression patterns upon target sequence binding. The other is a simple indirect mechanism whereby BRN2 levels are repressed with increasing MITF levels, thus reducing NOTCH pathway signalling through the absence of BRN2.

There have been few reports directly examining the degree, nature and consequences of melanoma tumour heterogeneity and the variation of cell morphology and immunohistochemical patterns within single melanocytic lesions of patients (Ohsie *et al.*, 2008), this is surprising given a direct relationship of melanogenesis and differentiation status of melanoma cells (Houghton *et al.*, 1987). For reasons of simplicity the melanoma field has pursued the relative homogenous nature of stable cell clones in adherent culture. Melanoma cell lines do possess an innate ability to respond to extracellular cues provided by the ECM and associated signalling molecules, with phenotypic switching apparent when introduced into an embryonic microenvironment illustrating the plasticity of these cells (Hendrix *et al.*, 2007). A recent model of melanoma progression has been put forward by Hoek and colleagues (2008) in which there is epigenetic switching of the gene expression pattern of cells from a proliferative to an invasive signature (Hoek *et al.*, 2008), moreover these are proposed to represent distinct yet interchangeable states which are regulated by signals from the microenvironment. The existence of two separate states within melanoma tumour xenografts studied in this work (Hoek *et al.*, 2008) was supported by histochemical staining for MITF and Ki67 antigens, which appeared higher in tumours derived from proliferative cell lines.

This association of MITF with the proliferative gene expression pattern has recently been supported by the finding of two distinct heterogeneous subpopulations within melanoma tumour biopsies as being largely MITF positive or negative. The more invasive fraction

being less proliferative and expressing low levels of MITF and high levels of $p27^{Kip1}$ (Carreira *et al.*, 2006). The ability of the BRN2 regulatory molecule (Cook and Sturm, 2008) to act as a direct repressor of the MITF gene promoter (Goodall *et al.*, 2008), combined with the discovery that MITF and BRN2 can be expressed in different subpopulations of cells within melanoma tumours, has lead to the hypothesis that individual cells may switch between BRN2+/MITF- and BRN2-/MITF+ states depending upon the extracellular cues. Alternatively this could be based on a stochastic mechanism in the absence of any signal (Dodd *et al.*, 2007), and that neither of these populations will reach clonal dominance within a tumour. Finally, remarkable images have recently been obtained using intravital microscopy to demonstrate that migrating B16-GFP tagged melanoma cells within tumours contain little or no pigment and high levels of BRN2 promoter activity (Pinner *et al.*, 2009), showing that it is a subset of undifferentiated melanoma cells that exit the primary tumour and give rise to the bulk of the resultant MITF positive differentiating cells during metastasis.

We have shown that melanoma cells grown in the adherent state or as short term spheroid-aggregates express high levels of both BRN2 and MITF unlike melanoma in situ. Induction of melanoma sphere formation and growth as tumour xenografts restores in part the BRN2+/MITF- or BRN2-/MITF+ reciprocal cellular expression patterns as seen in human melanoma tumours (Figure 3) (Goodall *et al.*, 2008). Our results demonstrate the importance of a BRN2-MITF axis of gene expression in efficient melanoma sphere formation as ablation of BRN2 results in poor sphere formation, and as we previously demonstrated a lack of ability to establish of tumours in mouse xenografts (Thomson *et al.*, 1995). Thus the study of melanoma sphere formation should provide a useful approach to gain insight into the processes that induce metastasis of melanoma. As a model, it is much more representative of melanoma in situ, and so potentially will provide more successful outcomes for novel drug

therapies than present models where results in vitro cannot be reproduced in the patient (Smalley *et al.*, 2006).

Materials and methods

Melanoma monolayer, sphere cell culture and spheroid formation

Human melanoma cell lines (listed in Supplementary Table 1) were maintained as a monolayer in MEL medium (RPMI 1640 medium supplemented with 2 % FBS, 3 % serum supreme, L- glutamine and pen strep). Melanoma sphere growth was induced by placing roughly 2.5 x 10^5 cells in a T25 flask in one of three types of medium; MEL medium, mouse embryonic fibroblast-conditioned human embryonic stem cell (hESC-KSR) medium (Fang *et al.*, 2005), or hESC-FBS medium (hESCM-KSR medium in which the Knockout Serum Supreme was replaced with 10 % FBS). The cultures were allowed to grow for a minimum of 14 days with media changes every second or third day and melanoma sphere formation was determined by the presence of floating clumps of 5 or more living cells using contrast microscopy (Supplementary Table 1). Floating spheres were passaged by mechanical disruption or enzymatic dissociation into single cell suspension and replated every 7-14 days. Adherent melanoma cells were induced to form 3D spheroid aggregates by liquid overlay onto Noble agar plates as described (Smalley *et al.*, 2006). Harvested floating spheres or aggregates were each imbedded into a gel of bovine collagen-1 as previously described (Smalley *et al.*, 2006) and left to invade in hESCM media for 72 hours.

TaqMan real-time PCR assay and siRNA transfection of adherent melanoma cells

Total cellular RNA was isolated and cDNA was prepared from monolayer and melanoma sphere cultures essentially as described (Smit *et al.*, 2007) and used for quantitative RT-PCR. Melanoma spheres were collected by spinning down the media to avoid collecting adherent cells. TaqMan probes for ABCB5 (Hs00698751_m1), BRN2 (Hs00271595_s1), DLL1 (Hs00194509_m1), GAPDH (Hs99999905_m1), JAG2 (Hs00171432_m1), MITF

(Hs00165156_m1), and NOTCH1 (Hs01062014_m1) (Applied Biosystems) were used as per manufacturers instructions using 50 ng cDNA. Data collection and analysis was performed using an ABI Prism 7500 (Applied Biosystems) with gene expression of averaged duplicate reactions normalized to either GAPDH or 18S ribosomal RNA.

Custom siRNA molecules (Ambion) specific to BRN2 (Cook *et al.*, 2005) and predesigned to MITF (No. 115142) (Newton *et al.*, 2007) were used in conjunction with a commercial negative control sequence (No. 4611) to monitor off-target effects. Transfections of MM96L cells were performed using 100 pmol of siRNA molecules using Lipofectamine 2000 and cells lysed after 48 hours as described (Smit *et al.*, 2007).

Protein analysis of cell extracts by Western immunoblot

Total cell extracts were collected from melanoma spheres and 80% confluent monolayer cultures and used for western immunoblotting as described previously (Cook *et al.*, 2003). Membranes were incubated with primary antibody for 1 hour at room temperature or overnight at 4° C at the following dilutions in 5% skim milk; anti-BRN2 1:500 (Smith *et al.*, 1998), anti-MITF 1:50 (Sigma), anti-NOTCH1 1:1000 (Sapphire Bioscience), anti-DLL1 1:500 (Sapphire Bioscience), anti-JAG2 1:1000 (Cell Signaling), and anti-glyceraldehyde-3-phosphate dehydrogenase 1:20000 (R&D Systems) as the loading control. The appropriate HRP-conjugated secondary antibody diluted in 3% skim milk 1:8000 to 1:10000 (ZyMed) was incubated with membranes for 1 hour at room temperature and membranes were visualized using Immobulin Western (Millipore).

Immunofluoresence microscopy

Melanoma spheres were collected and rinsed in PBS twice before incubation in 4% paraformaldehyde for 1 hour at room temperature. After two rinses in PBS, the spheres were embedded in O.C.T. (Tissue-Tek) and cut into 10 µm sections using a Leica cryostat CM3050 S. Cells were permeabalised by incubation in 0.1 % Triton X for 10 min, rinsed in

0.5 % BSA in PBS 2 x 10 min, and incubated with primary antibody overnight at 4° C. Antibodies were used at the following dilutions, BRN2 1:50, MITF 1:50, NOTCH1 1:100, JAG2 1:100, and DLL1 1:100 were all diluted in 0.5 % BSA in PBS, except for xenograft samples for which a M.O.M. blocking kit was utilised (Vector Laboratories, Cat# BMK-2202) as per instructions. After 3 x 10 min washes in 0.5 % BSA in PBS, sections were incubated in corresponding anti-rabbit or anti-mouse Alexa Fluor 594- or 488-conjugated secondary antibody 1:200 for 1 hour at room temperature and again washed 3 x 10 min 0.5 % BSA in PBS. Finally, the sections were incubated in DAPI 1:1000 for 10 min and staining was observed using confocal microscopy and standard fluorescence microscopy. Monolayer cells were plated on glass coverslips, fixed in 4% paraformaldehyde and stained as described previously using the same antibody dilutions as above (Cook *et al.*, 2003).

Mouse xenografts, human tissue samples, antigen retrieval, and H&E staining

Attached melanoma cells were harvested by enzymatic digestion and melanoma spheres were pelleted from the media and washed in PBS. Matched adherent and sphere preparations were injected into the left and right flank, respectively, of 4 week old NOD/SCID IL2g-/- mice. Five mice per group were injected intradermally with 200,000 or 20,000 cells in 100 µl of Matrigel per injection site. The mice were sacrificed in groups according to when one mouse in each group yielded a tumour size of 0.5 cm^3. Tumours were excised, fixed in formalin, transferred to ethanol then embedded in paraffin. Blocks were processed for staining and antibody binding as per below.

Primary human superficial spreading melanoma tissues removed from a 78 year old with a facial lesion were obtained as formalin-fixed, paraffin-embedded blocks and cut as serial whole 10µm transverse cross sections (Richmond-Sinclair *et al.*, 2008). Sections were deparaffinised in xylene and rehydrated in an ethanol gradient prior to antigen retrieval. These were heated to 125 degrees Celsius, for 4 min in a 10mM citrate buffer pH 6.0 (Vector Laboratories, cat# H-3300) using an antigen decloaking chamber (Biocare Medical Model#

DC2002). The sections were then microwaved (600W) twice, for 8 min each, with a fresh citrate buffer change between heating cycles, then cooled to room temperature prior to antibody labeling. 10μm tumour serial sections were deparaffinised in xylene, rehydrated in an ethanol gradient series, treated with hemotoxylin for 3 min, rinsed in concentrated HCl, partially dehydrated in ethanol, treated with eosin for 20 sec and dehydrated in an ethanol gradient series prior to being mounted with Entellan (Pro Sci Tech cat# IM022). All experiments were undertaken with the approval of the University of Queensland research ethics committee.

Conflict of interest

The authors declare no conflict of interest.

Acknowledgements

We thank Prof. N. Hayward (QIMR) for providing some of the cell lines that were tested for melanoma sphere formation as part of this manuscript. RAS is a Senior Research Fellow of the Australian NHMRC and in conducting part of this work was supported by an SSP award from the University of Queensland. This work was supported by grants from the Cancer Council Queensland to RAS and JHL and NIH grant CA-25874 to MH.

References

Alonso SR, Tracey L, Ortiz P, Perez-Gomez B, Palacios J, Pollan M *et al* (2007). A high-throughput study in melanoma identifies epithelial-mesenchymal transition as a major determinant of metastasis. *Cancer Res* **67:** 3450-3460.

Carreira S, Goodall J, Denat L, Rodriguez M, Nuciforo P, Hoek KS *et al* (2006). Mitf regulation of Dia1 controls melanoma proliferation and invasiveness. *Genes Dev* **20:** 3426-3439.

Castro DS, Skowronska-Krawczyk D, Armant O, Donaldson IJ, Parras C, Hunt C *et al* (2006). Proneural bHLH and Brn proteins coregulate a neurogenic program through cooperative binding to a conserved DNA motif. *Dev Cell* **11:** 831-844.

Cook AL, Boyle GM, Leonard JH, Parsons PG, Sturm RA (2006). BRN2 in melanocytic cell development, differentiation and transformation. In: Hearing VJ and Leong SPL (eds). *From Melanocytes to Melanoma*. Humana Press: Totowa, New Jersey. pp 149-167.

Cook AL, Donatien PD, Smith AG, Murphy M, Jones MK, Herlyn M *et al* (2003). Human melanoblasts in culture: expression of BRN2 and synergistic regulation by fibroblast growth factor-2, stem cell factor, and endothelin-3. *J Invest Dermatol* **121:** 1150-1159.

Cook AL, Smith AG, Smit DJ, Leonard JH, Sturm RA (2005). Co-expression of SOX9 and SOX10 during melanocytic differentiation in vitro. *Exp Cell Res* **308:** 222-235.

Cook AL, Sturm RA (2008). POU domain transcription factors: BRN2 as a regulator of melanocytic growth and tumourigenesis. *Pigment Cell Melanoma Res* **21:** 611-626.

Dodd IB, Micheelsen MA, Sneppen K, Thon G (2007). Theoretical analysis of epigenetic cell memory by nucleosome modification. *Cell* **129:** 813-822.

Fang D, Nguyen TK, Leishear K, Finko R, Kulp AN, Hotz S *et al* (2005). A tumorigenic subpopulation with stem cell properties in melanomas. *Cancer Res* **65:** 9328-9337.

Goodall J, Carreira S, Denat L, Kobi D, Davidson I, Nuciforo P *et al* (2008). Brn-2 represses microphthalmia-associated transcription factor expression and marks a distinct subpopulation of microphthalmia-associated transcription factor-negative melanoma cells. *Cancer Res* **68:** 7788-7794.

Hendrix MJ, Seftor EA, Seftor RE, Kasemeier-Kulesa J, Kulesa PM, Postovit LM (2007). Reprogramming metastatic tumour cells with embryonic microenvironments. *Nat Rev Cancer* **7:** 246-255.

Hoek KS, Eichhoff OM, Schlegel NC, Dobbeling U, Kobert N, Schaerer L *et al* (2008). In vivo switching of human melanoma cells between proliferative and invasive states. *Cancer Res* **68:** 650-656.

Houghton AN, Real FX, Davis LJ, Cordon-Cardo C, Old LJ (1987). Phenotypic heterogeneity of melanoma. Relation to the differentiation program of melanoma cells. *J Exp Med* **165:** 812-829.

Johansson P, Pavey S, Hayward N (2007). Confirmation of a BRAF mutation-associated gene expression signature in melanoma. *Pigment Cell Res* **20:** 216-221.

Mani SA, Guo W, Liao MJ, Eaton EN, Ayyanan A, Zhou AY *et al* (2008). The epithelial-mesenchymal transition generates cells with properties of stem cells. *Cell* **133:** 704-715.

Miller AJ, Mihm MC, Jr. (2006). Melanoma. *N Engl J Med* **355:** 51-65.

Na YR, Seok SH, Kim DJ, Han JH, Kim TH, Jung H *et al* (2009a). Isolation and Characterization of Spheroid Cells from Human Malignant Melanoma Cell Line WM-266-4. *Tumour Biol* **30:** 300-309.

Na YR, Seok SH, Kim DJ, Han JH, Kim TH, Jung H *et al* (2009b). Zebrafish embryo extracts promote sphere-forming abilities of human melanoma cell line. *Cancer Sci* **100:** 1429-1433.

Newton RA, Cook AL, Roberts DW, Leonard JH, Sturm RA (2007). Post-transcriptional regulation of melanin biosynthetic enzymes by cAMP and resveratrol in human melanocytes. *J Invest Dermatol* **127:** 2216-2227.

Ohsie SJ, Sarantopoulos GP, Cochran AJ, Binder SW (2008). Immunohistochemical characteristics of melanoma. *J Cutan Pathol* **35:** 433-444.

Pavey S, Johansson P, Packer L, Taylor J, Stark M, Pollock PM *et al* (2004). Microarray expression profiling in melanoma reveals a BRAF mutation signature. *Oncogene* **23:** 4060-4067.

Pinner S, Jordan P, Sharrock K, Bazley L, Collinson L, Marais R *et al* (2009). Intravital imaging reveals transient changes in pigment production and Brn2 expression during metastatic melanoma dissemination. *Cancer Res* **69:** 7969-7977.

Pinnix CC, Herlyn M (2007). The many faces of Notch signaling in skin-derived cells. *Pigment Cell Res* **20:** 458-465.

Pinnix CC, Lee JT, Liu ZJ, McDaid R, Balint K, Beverly LJ *et al* (2009). Active Notch1 confers a transformed phenotype to primary human melanocytes. *Cancer Res* **69:** 5312-5320.

Quintana E, Shackleton M, Sabel MS, Fullen DR, Johnson TM, Morrison SJ (2008). Efficient tumour formation by single human melanoma cells. *Nature* **456:** 593-598.

Richmond-Sinclair NM, Lee E, Cummings MC, Williamson R, Muller K, Green AC *et al* (2008). Histologic and epidemiologic correlates of P-MAPK, Brn-2, pRb, p53, and p16 immunostaining in cutaneous melanomas. *Melanoma Res* **18:** 336-345.

Schatton T, Murphy GF, Frank NY, Yamaura K, Waaga-Gasser AM, Gasser M *et al* (2008). Identification of cells initiating human melanomas. *Nature* **451:** 345-349.

Smalley KS, Haass NK, Brafford PA, Lioni M, Flaherty KT, Herlyn M (2006). Multiple signaling pathways must be targeted to overcome drug resistance in cell lines derived from melanoma metastases. *Mol Cancer Ther* **5:** 1136-1144.

Smit DJ, Gardiner BB, Sturm RA (2007). Osteonectin downregulates E-cadherin, induces osteopontin and focal adhesion kinase activity stimulating an invasive melanoma phenotype. *Int J Cancer* **121:** 2653-2660.

Smith AG, Brightwell G, Smit SE, Parsons PG, Sturm RA (1998). Redox regulation of Brn-2/N-Oct-3 POU domain DNA binding activity and proteolytic formation of N-Oct-5 during melanoma cell nuclear extraction. *Melanoma Res* **8:** 2-10.

Thomson JAF, Murphy K, Baker E, Sutherland GR, Parsons PG, Sturm RA (1995). The brn-2 gene regulates the melanocytic phenotype and tumorigenic potential of human melanoma cells. *Oncogene* **11:** 691-700.

Figure legends

Figure 1. Melanoma sphere induction in human melanoma cell lines. A and B. A11 and D10 cell lines were plated as adherent monolayers and grown to confluence in T75 flasks before changing to the media indicated above the panels as MEL, hESCM-FBS or hESCM-KSR. Digital pictures were taken of cells under bright field microscopy on the days as indicated to the right of the panels (D4, D6, D9, D13). Floating cell aggregates were harvested from the flasks at D14 or earlier and passaged as melanoma spheres as described. Scale bars in black represent 200 microns. **C.** Loss of pigmentation in A11 melanoma cells was apparent upon changing from adherent to detached growth states. The colour of the cell pellets from adherent cells (P0) and those from serially passaged melanoma spheres in hESCM-KSR medium (P1, P2, P3) demonstrates the cells becoming amelanotic.

Figure 2. Regulatory protein changes between adherent and melanoma sphere cell growth. A. Individual western blot filters of total protein lysates prepared from A2058 (lanes 1, 2), A11 (lanes 3, 4) and MM96L (lanes 5, 6) cell lines grown as adherent (A) or melanoma spheres (S) were probed with the antibodies indicated to the left of each panel. The loading control was GAPDH. **B.** Quantitative RT-PCR was performed on total RNA extracted from adherent (A) or melanoma spheres (S) to determine the expression level of BRN2, MITF, NOTCH1, JAG2, DLL1 and ABCB5. Levels were normalized to GAPDH and plotted as histograms in relative expression units, with the bars showing the range of expression. **C.** A2058 cells grown as adherent or as melanoma spheres were either fixed on cover slips or prepared as sections respectively. Immunofluorescence microscopy was performed on these samples using antibodies to NOTCH1, JAG2 and DLL1 proteins as indicated above the panels. The blue DAPI stain highlights the nucleus of each cell. A difference in JAG2 expression intensity relative to the DAPI stained nuclei can be seen in the centre panel. Scale bars in white represent 20 microns.

Figure 3. Heterogeneous BRN2 and MITF expression patterning in melanoma and melanoma models. A. Immunofluorescence microscopy of BRN2 (red) and MITF (green) costained adherent cells, agar spheroid aggregates and melanoma spheres in three different cell lines, A2058, A11 and MM96L. Spheroid aggregates and spheres were fixed in 4% PFA, imbedded in OCT thermal compound, cryosectioned and antigen retrieved prior to labelling with antibody. Scale bars in white represent 100 microns. **B**. Immunofluorescent BRN2 (red) and MITF (green) costaining of human cell lines WM3437 and WM115 induced to grow as melanoma tumour xenografts on the flanks of immunocompromised mice. H&E histology stains were conducted to gain structural and morphological context were cut in serial section from samples presented for immunofluorescence. Scale bars in white represent 100 microns. **C**. Immunofluorescent BRN2 (red) and MITF (green) costaining of a human primary facial superficial spreading melanoma. The tumour was surgically removed, formalin fixed, paraffin imbedded, sectioned at 10μM, and antigen retrieved prior to antibody labelling. Scale bars in white represent 500 or 100 microns (zoomed section). The region presented at greater magnification is boxed.

Figure 4. Gene expression patterns upon BRN2 and MITF repression and melanoma sphere formation. A and B. Cultures of MM96L and A2058 grown as adherent cells were separately treated with siRNA directed against BRN2 (B), MITF (M) and a negative control sequence (C), 48 hours later cells were assessed for the expression of the genes indicated above each graph by quantitative RT-PCR with levels normalised relative to 18S RNA. **C.** Total protein extracts from the same siRNA treated cells as indicated in parts A and B were subject to western immunoblot with the antibodies indicated to the left of each panel, GAPDH serving as the loading control.

Figure 5. Ablation of BRN2 inhibits sphere formation and invasion, and alters the expression of downstream targets. A. Melanoma spheres at 31 days post induction are

shown with the field representative of a random 5% of the area occupied by the total spheres per cell line over this time period. Sphere count contained in a 100µl aliquot of low speed pelleted media per cell line. After observing sphere formation and density by light microscopy spheres were counted at days 11, 13 and 15 for clone 10 and days 25, 27 and 29 for clone 8. Scale bars in black represent 200 microns. **B**. Agar spheroid bright field light microscopy images (4X objective) at 72 hours post induction. Scale bars in black represent 200 microns. **C.** Sphere cells invading though collagen (4X objective). Spheres were imbedded in collagen and incubated for 72 hours in hESCM media. MM96L parent line shows good outgrowth of cells from the sphere, with little outgrowth observed for the low contrast MM96Lc10LC (10LC) and no outgrowth for the MM96Lc8LC (8LC) clones. Scale bars in black represent 100 microns. **D.** Total protein lysates prepared from MM96L parental (P) (lanes 1, 2), MM96Lc8D (lanes 3, 4), MM96Lc8LC (lanes 5, 6), MM96Lc10D (lanes 7, 8) and MM96Lc10LC (lanes 9, 10), with cell strains grown as adherent (A) or melanoma spheres (S), were probed with the antibodies indicated to the left of each panel. GAPDH was used as a loading control.

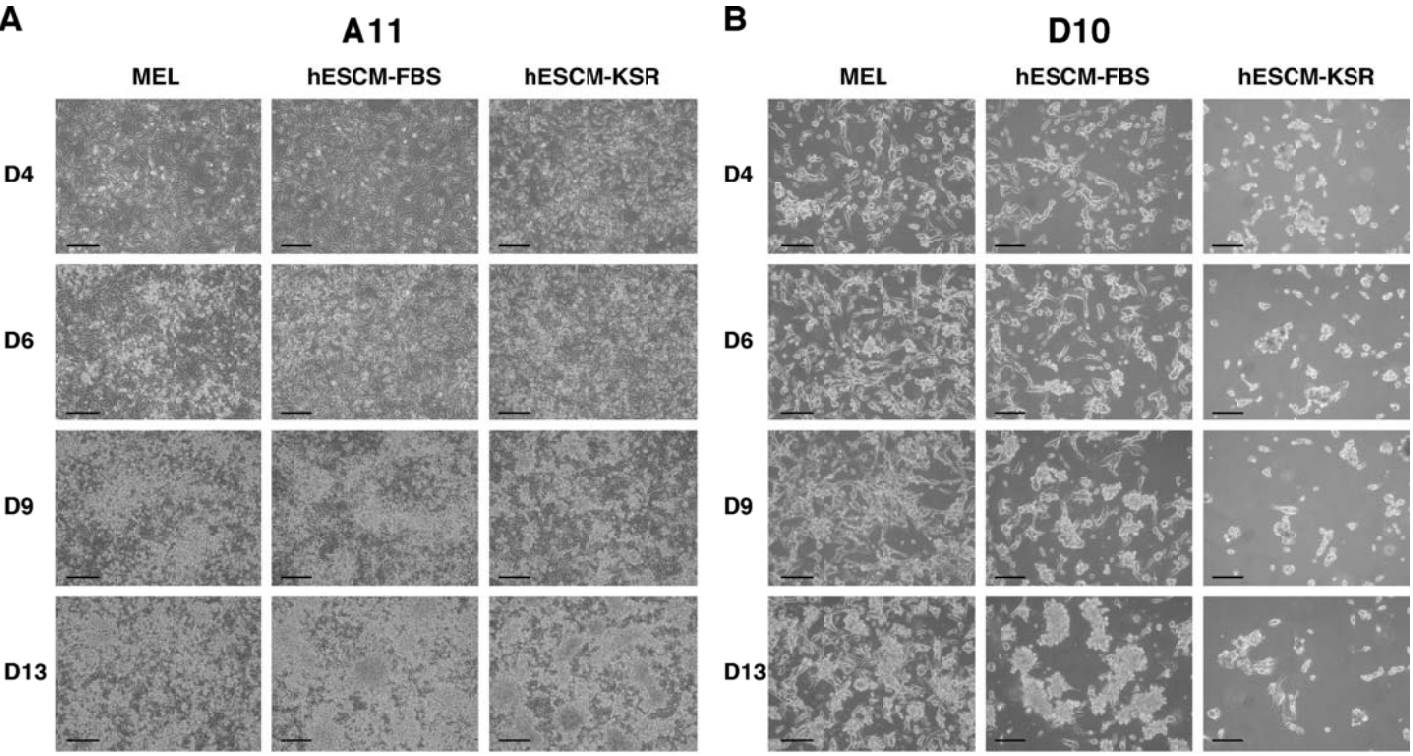
A
A11
MEL
hESCM-FBS
hESCM-KSR
D4
D6
D9
D13
B
D10
MEL
hESCM-FBS
hESCM-KSR
D4
D6
D9
D13

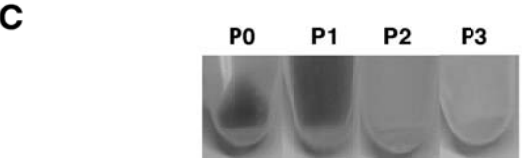
C
P0
P1
P2
P3

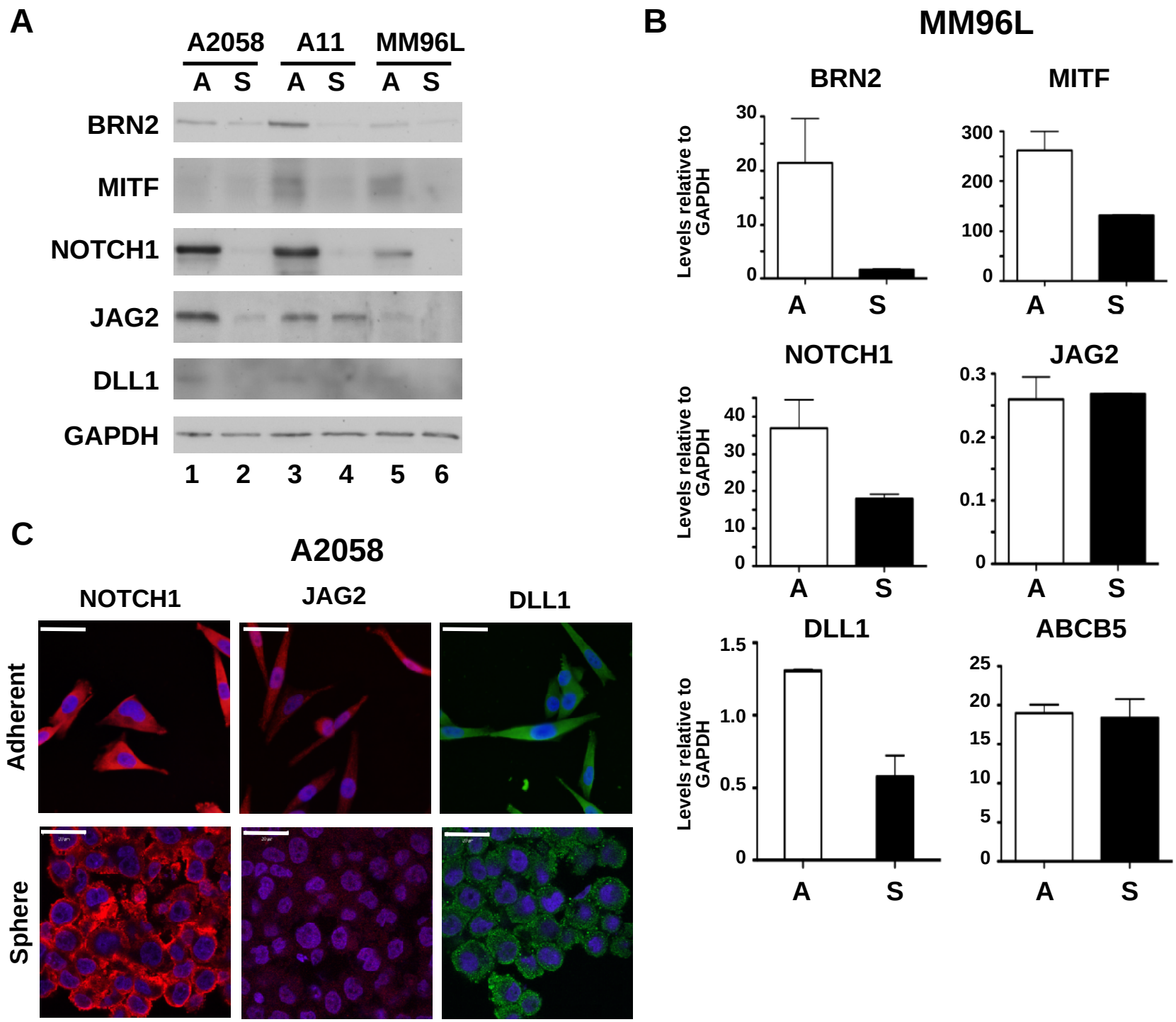
A
A2058
A11
MM96L
A S A S A S
BRN2
MITF
NOTCH1
JAG2
DLL1
GAPDH
1 2 3 4 5 6
B
MM96L
BRN2
MITF
NOTCH1
JAG2
DLL1
ABCB5
Levels relative to GAPDH
A
S
C
A2058
NOTCH1
JAG2
DLL1
Adherent
Sphere

A

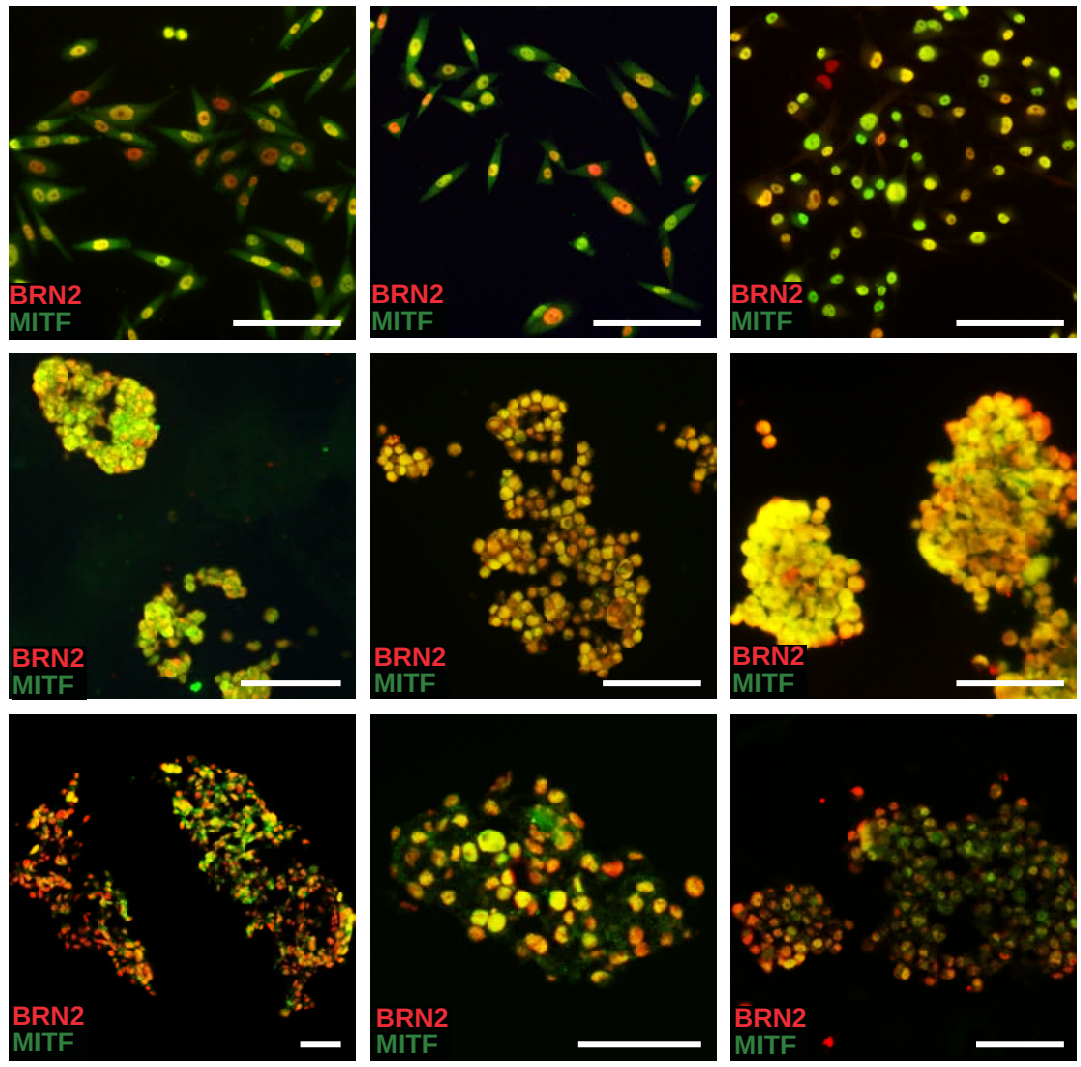
A2058
A11
MM96L
Adherent
Agar Spheroid
Sphere
BRN2
MITF

B

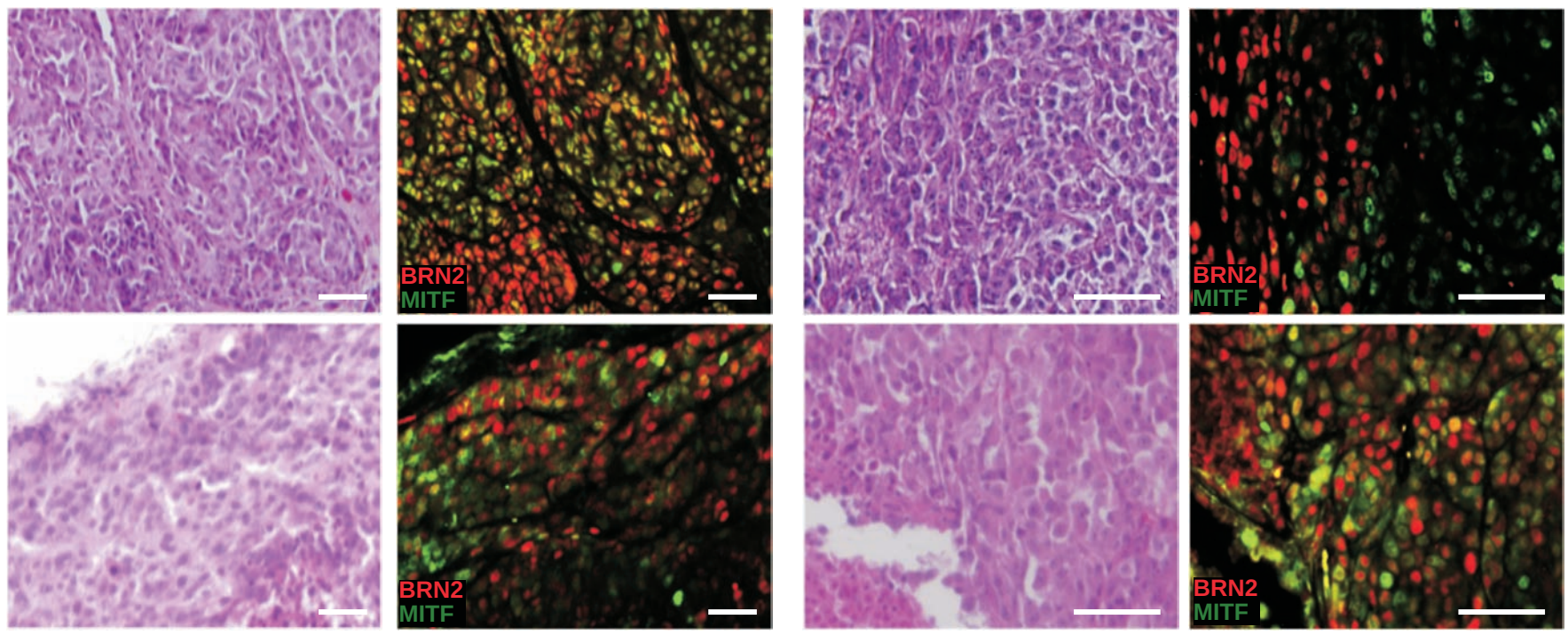
Mouse Xenograft
WM3734
WM115
Adherent
Sphere
BRN2
MITF

C

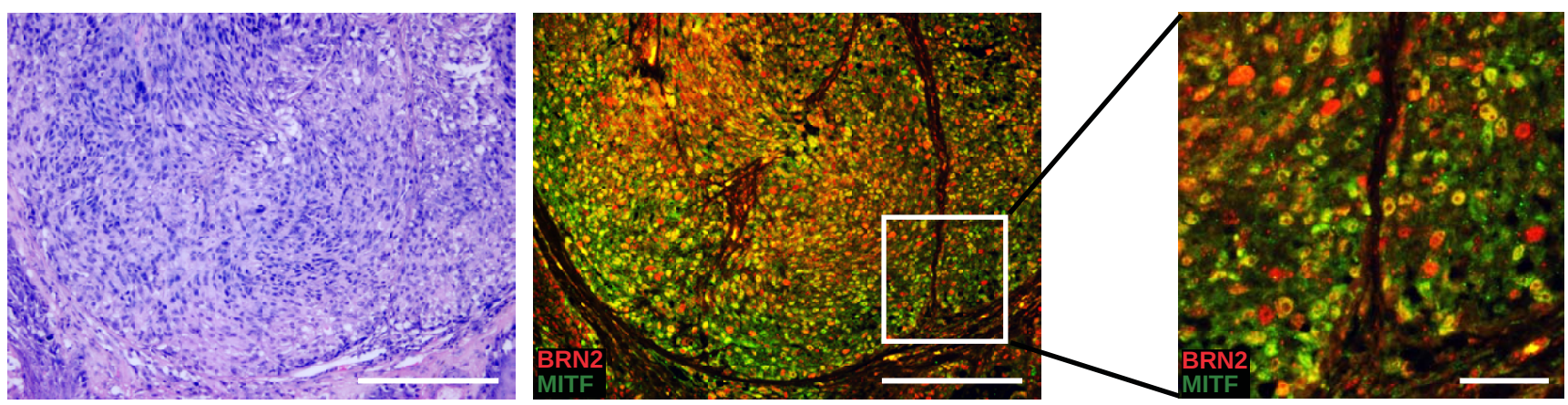
Human MelanomaTumour
BRN2
MITF

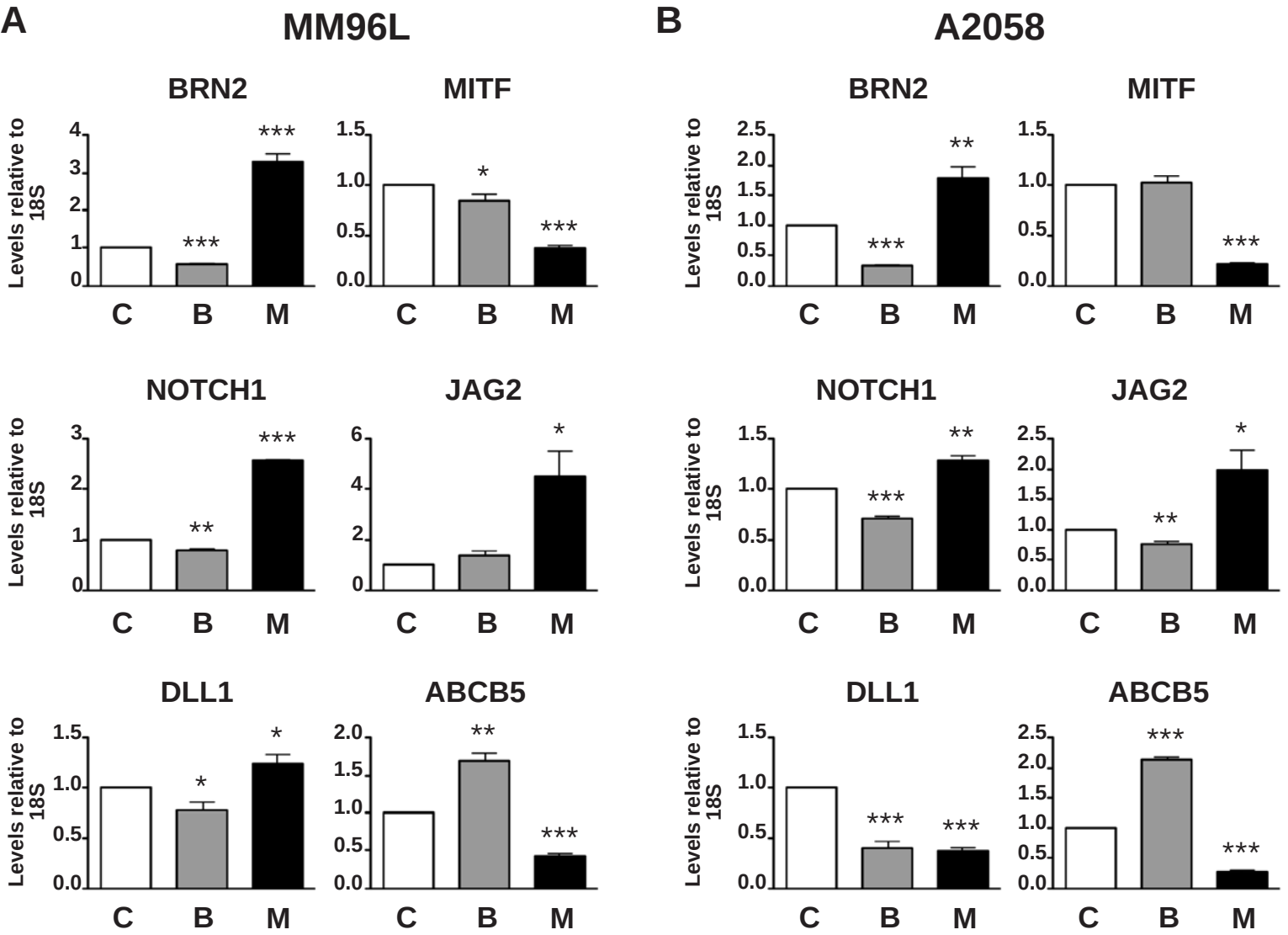
A
MM96L
BRN2
MITF
NOTCH1
JAG2
DLL1
ABCB5
Levels relative to 18S
C
B
M
B
A2058
BRN2
MITF
NOTCH1
JAG2
DLL1
ABCB5
Levels relative to 18S
C
B
M

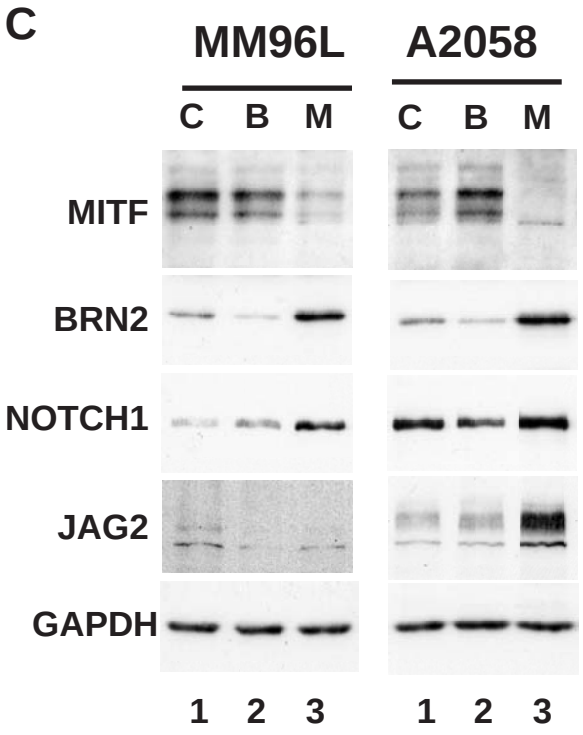
C
MM96L
A2058
C B M
C B M
MITF
BRN2
NOTCH1
JAG2
GAPDH
1 2 3
1 2 3

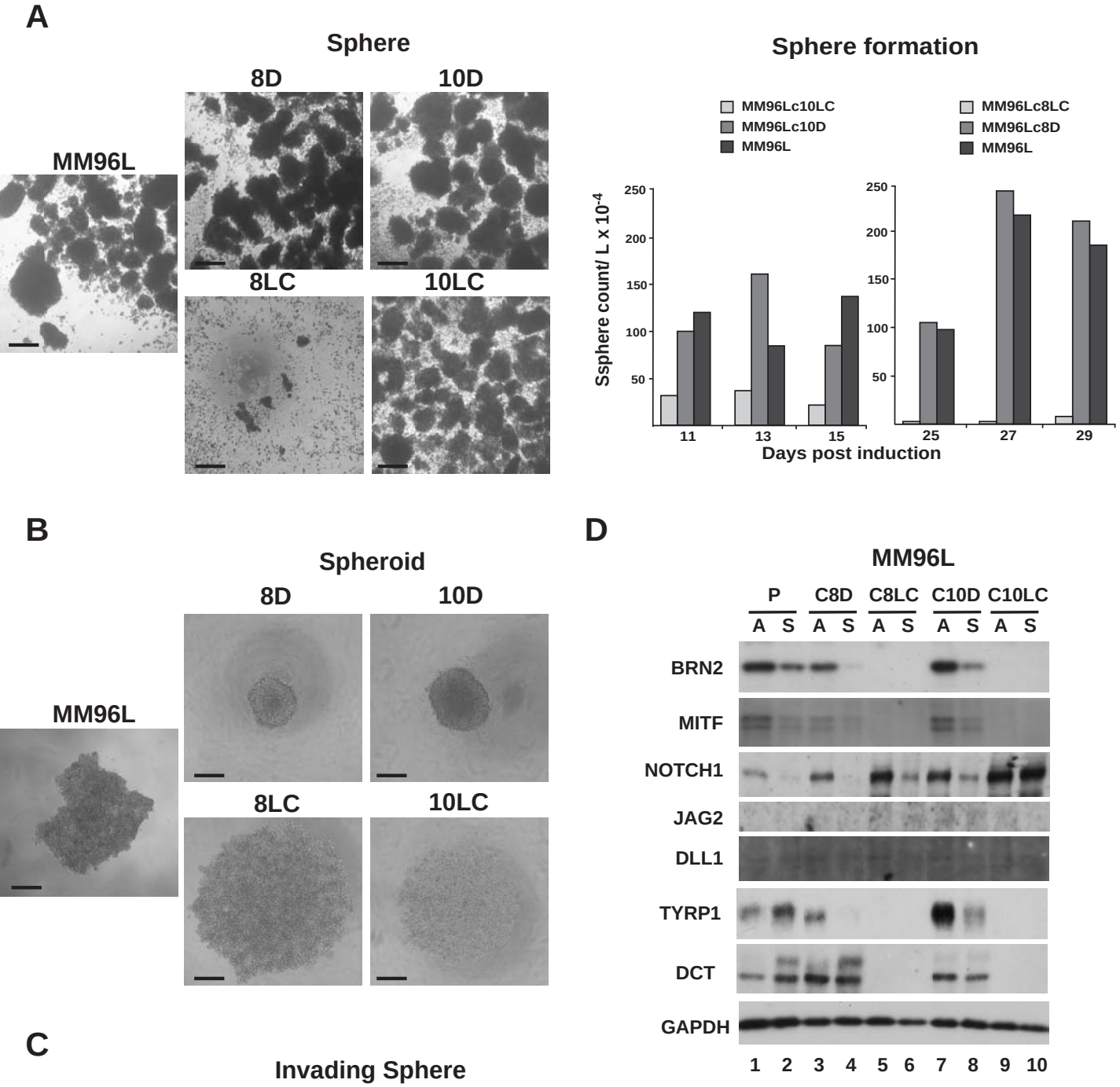
A
Sphere
8D
10D
MM96L
8LC
10LC
Sphere formation
MM96Lc10LC
MM96Lc10D
MM96L
MM96Lc8LC
MM96Lc8D
MM96L
Ssphere count/ L x 10-4
250
200
150
100
50
11
13
15
25
27
29
Days post induction
B
Spheroid
8D
10D
MM96L
8LC
10LC
C
Invading Sphere
8D
10D
MM96L
8LC
10LC
D
MM96L
P
C8D
C8LC
C10D
C10LC
A S A S A S A S A S
BRN2
MITF
NOTCH1
JAG2
DLL1
TYRP1
DCT
GAPDH
1 2 3 4 5 6 7 8 9 10